J|A|C|S ARTICLES

Published on Web 05/07/2010

Binding or Bending: Distinction of Allosteric Abl Kinase Agonists from Antagonists by an NMR-Based Conformational Assay

Wolfgang Jahnke,* Robert M. Grotzfeld, Xavier Pellé, André Strauss, Gabriele Fendrich, Sandra W. Cowan-Jacob, Simona Cotesta, Doriano Fabbro, Pascal Furet, Jürgen Mestan, and Andreas L. Marzinzik

Novartis Institutes for Biomedical Research, 4002 Basel, Switzerland

Received March 4, 2010; E-mail: wolfgang.jahnke@novartis.com

Abstract: Allosteric inhibitors of Bcr-Abl have emerged as a novel therapeutic option for the treatment of CML. Using fragment-based screening, a search for novel Abl inhibitors that bind to the myristate pocket was carried out. Here we show that not all myristate ligands are functional inhibitors, but that the conformational state of C-terminal helix_I is a structural determinant for functional activity. We present an NMR-based conformational assay to monitor the conformation of this crucial helix_I and show that myristate ligands that bend helix_I are functional antagonists, whereas ligands that bind to the myristate pocket but do not induce this conformational change are kinase agonists. Activation of c-Abl by allosteric agonists has been confirmed in a biochemical assay.

Introduction

Under normal circumstances, the enzymatic activity of c-Abl kinase is tightly regulated. This is in part due to myristoyl-mediated autoinhibition:[1] In c-Abl isoform 1b, a myristoyl group covalently attached to Gly2 at the N-terminus can bind to a deep pocket within the kinase domain,[2] which causes the SH2 and SH3 domains to dock against the kinase domain, thereby forming an assembled inactive state (Figure 1a,b).[2] The oncogenic fusion protein, Bcr-Abl, lacks the myristoylation site of c-Abl 1b. It is constitutively active and transforms hematologic stem cells to cause chronic myelogenous leukemia (CML).[3] Although drugs targeting Bcr-Abl, such as imatinib, nilotinib, or dasatinib, are efficacious treatments of CML, they all bind within the ATP pocket of the Abl kinase domain, and advanced patients can relapse due to the emergence of resistance mutations.[4]

Myristate mimetics capable of stabilizing Bcr-Abl in the assembled inactive state could function as allosteric inhibitors of Bcr-Abl. Since they bind at a different pocket, such compounds could be active against mutant enzymes resistant to ATP-site inhibitors. Differential cytotoxicity screening has led to the discovery of GNF-2, which is a highly selective Abl inhibitor[5] and has been shown to bind to the myristate pocket.[6] However, GNF-2 is based on an aminopyrimidine scaffold well-known for its ability to bind to the hinge region in the ATP pocket of kinases. In order to fully exploit the potential of the nonconserved myristoyl binding pocket on Abl, we applied fragment-based screening to identify alternative scaffolds that inhibit the kinase. In the course of fragment screening, characterization, and optimization, we gained insights into the structural requirements and conformational changes that myristate ligands have to induce in order to be functional inhibitors. We developed an NMR-based conformational assay to rapidly monitor the ability of myristate ligands to bend helix_I, which is a prerequisite for functional activity. Finally, we reason that myristate ligands that bind but do not bend helix_I should be allosteric agonists of c-Abl kinase. We prove this hypothesis in a biochemical c-Abl assay and discuss the potential utility of c-Abl (not Bcr-Abl) activators.

Experimental Section

Nomenclature. ABL1 is referred to as c-Abl, BCR-ABL1 is referred to as Bcr-Abl. Residues are numbered according to the c-Abl 1b isoform.

Protein Expression and Purification. For NMR: Murine c-Abl (248-534, Abl 1b numbering) was expressed with ^{15}N-valine and purified as previously described.[7] Murine c-Abl and human c-Abl differ only in three positions (N355 → S355, Q532 → R532, V534 → T534 for human → mouse), neither of which is expected to affect the myristate pocket. The cost for the ^{15}N-valine isotopes for the production of 8 mg of ^{15}N-Val-Abl (sufficient for 20 samples) was below $100. The buffer used for NMR studies was 20 mM Bis-Tris (pH 6.5), 150 mM NaCl, 1 mM EDTA, 2 mM TCEP. For X-ray: Murine c-Abl (248-534, Abl 1b numbering) was expressed in the presence of imatinib (received from the Novartis compound archive) and purified as previously described.[6] The Abl/imatinib complex (molar ratio 1:1) was concentrated to 20 mg/mL in 20

(1) Hantschel, O.; Nagar, B.; Guettler, S.; Kretzschmar, J.; Dorey, K.; Kuriyan, J.; Superti-Furga, G. *Cell* **2003**, *112* (6), 845–857.
(2) Nagar, B.; Hantschel, O.; Young, M. A.; Scheffzek, K.; Veach, D.; Bornmann, W.; Clarkson, B.; Superti-Furga, G.; Kuriyan, J. *Cell* **2003**, *112* (6), 859–871.
(3) Ren, R. *Nat. Rev. Cancer* **2005**, *5* (3), 172–183.
(4) O'Hare, T.; Eide, C. A.; Deininger, M. W. *Blood* **2007**, *110* (7), 2242–2249.
(5) Adrian, F. J.; Ding, Q.; Sim, T.; Velentza, A.; Sloan, C.; Liu, Y.; Zhang, G.; Hur, W.; Ding, S.; Manley, P.; Mestan, J.; Fabbro, D.; Gray, N. S. *Nat. Chem. Biol.* **2006**, *2* (2), 95–102.
(6) Zhang, J.; et al. *Nature* **2010**, *463* (7280), 501–506.
(7) Strauss, A.; Bitsch, F.; Cutting, B.; Fendrich, G.; Graff, P.; Liebetanz, J.; Zurini, M.; Jahnke, W. *J. Biomol. NMR* **2003**, *26* (4), 367–372.

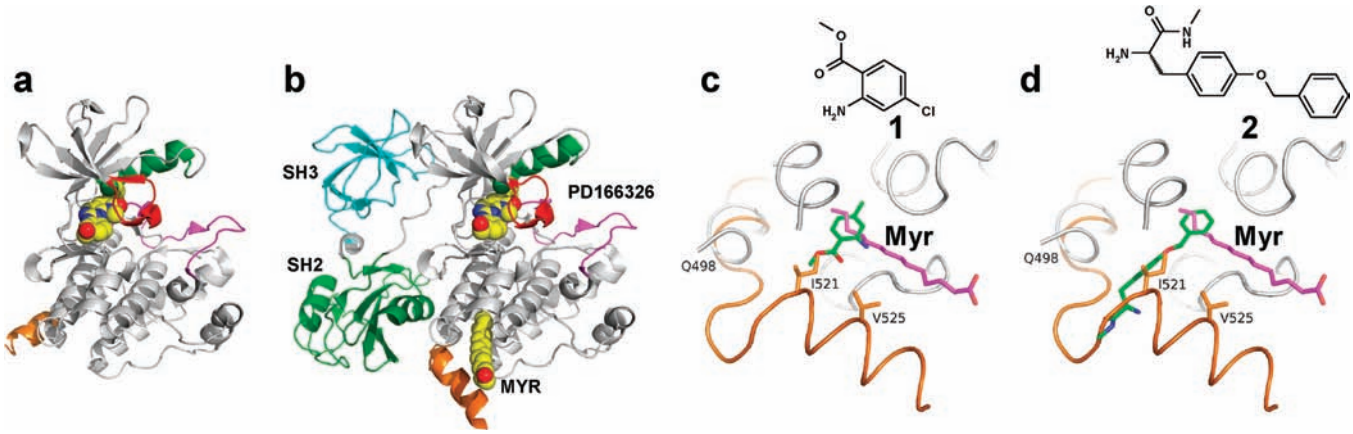

Figure 1. Crystal structures of c-Abl complexes. (a) In the absence of a ligand for the myristate pocket, helix_I (orange) is straight (PDB code 2G2H[20]). (b) In the presence of myristate, helix_I is bent and the SH2 and SH3 domains dock against the kinase domain (PDB code 1OPK[2]). (c,d) Details of the myristate pocket in complex with fragments 1 and 2, shown above. The position of myristate is superimposed for illustration only. Similarly, helix_I is not visible in the structures shown in c and d, but for illustration, its position in 1OPK is superimposed. Note the steric clash that would occur if helix_I adopted this bent conformation. The color code is orange for helix_I, magenta for myristate, green for helix_C and fragments 1 and 2, red for the P-loop, and pink for the activation loop. The ATP binding site of c-Abl is filled with PD166326 in a and b, and with imatinib in c and d.

mM Tris-HCl, 100 mM NaCl, 1 mM EDTA, pH 7.6 plus 4 mM DTT before crystallization.

NMR Spectroscopy. All NMR experiments were carried out on a Bruker AV600 spectrometer at a proton frequency of 600 MHz using a TCI cryoprobe. For the conformational assay, HSQC spectra were recorded using ^{15}N-Val-Abl at a concentration of 1.4 mg/mL (44 μM) and a volume of 200 μL. The temperature was 296 K; 160 increments of 80 scans each were recorded, resulting in a measuring time of 5 h. Shorter measuring times can be used if the Abl concentration is appropriately raised.

Determination of Dissociation Constants. Dissociation constants (K_D) were measured by NMR in one or both of the following ways.

(1) Direct titration of Abl/imatinib complex with increasing amounts of ligand by ^{1}H NMR: A methyl group from a residue lining the myristate binding pocket has a resonance at -0.16 ppm, which is nonoverlapping in a 1D ^{1}H spectrum and is sensitive to the presence of a ligand. The chemical shift of this methyl group was followed as ligand was added. The titration curve follows a simple exponential and can be interpreted as percentage of bound protein as a function of ligand concentration. From this curve, the dissociation constant, K_D, is easily extracted by curve fitting using the program Origin 7.5. Supporting Information Figure 1 shows sample spectra and sample titration curves for three different fragments.

(2) Competition experiments: Binding affinity of a test compound was measured by its ability to displace a reporter ligand with known binding affinity, such as compound **1** (refs 8 and 9). Twenty compounds for which the dissociation constant had been determined by direct titration were used to experimentally calibrate the displacement curve. After calibration, dissociation constants determined by direct titration or by competition experiments generally agreed within a factor of 3.

For selected compounds, the dissociation constants were also determined by isothermal titration calorimetry (ITC). The ITC-derived values were identical within a factor of 2 to the values derived from direct NMR titration.

^{15}N-Val Resonance Assignments of Abl/imatinib Complex. Almost complete backbone resonance assignment for the Abl/imatinib complex has previously been achieved,[10] and the assignments have been deposited with the BioMagResBank (BMRB submission code 15488). The human Abl construct for resonance assignment ended at residue Ser519, while the mouse Abl construct used for this work extended up to Thr534. Val525 is the only valine residue that is added in the longer construct, and its chemical shift was thus easily assigned to 7.95 ppm (^{1}H) and 120.7 ppm (^{15}N).

Crystal Structure Determination. For the complex with fragment **1**, crystals were obtained by cocrystallization in the presence of an excess of the fragment using the method of hanging drop vapor diffusion and a reservoir solution consisting of 0.1 M MES pH 6.5, 0.2 M magnesium chloride, and 18.4% PEG4000 at 4 °C. The crystals used for soaking with fragment **2** were obtained by hanging drop vapor diffusion using a reservoir consisting of 0.1 M imidazole pH 6.5, 0.2 M magnesium chloride, 2% ethylene glycol, 13.8% PEG4000 at 4 °C. The latter crystals were soaked overnight at 4 °C in a 2.5 mM solution of fragment **2** in the crystallization buffer. In both cases, the crystals were then transferred in the same buffer containing gradually increasing concentrations of ethylene glycol and flash cooled in liquid nitrogen when the concentration reached 20%.

Diffraction data were collected from single crystals at beamline PXII of the Swiss Light Source (wavelength 0.9999 Å, Supporting Information Table 1). For fragment **1**, a complete data set was collected using a MARCCD 225 after 161° of rotation with 1° rotation ranges for each image. For fragment **2**, 100° of data was collected in the same way. All data were processed inside APRV[11] using XDS.[12] The structure of the complex with fragment **1** was solved using molecular replacement with the program MOLREP.[13] The structure with fragment **2** was solved using rigid body refinement and difference Fourier methods with Refmac5[14] and the protein coordinates of PDB entry 1OPJ[2] as a starting model. In both cases, refinement proceeded with cycles of model building

(8) Dalvit, C.; Flocco, M.; Knapp, S.; Mostardini, M.; Perego, R.; Stockman, B. J.; Veronesi, M.; Varasi, M. *J. Am. Chem. Soc.* **2002**, *124* (26), 7702–7709.
(9) Jahnke, W.; Floersheim, P.; Ostermeier, C.; Zhang, X.; Hemmig, R.; Hurth, K.; Uzunov, D. P. *Angew. Chem., Int. Ed.* **2002**, *41* (18), 3420–3423.
(10) Vajpai, N.; Strauss, A.; Fendrich, G.; Cowan-Jacob, S. W.; Manley, P. W.; Jahnke, W.; Grzesiek, S. *Biomol NMR Assign* **2008**, *2* (1), 41–42.
(11) Kroemer, M.; Dreyer, M. K.; Wendt, K. U. *Acta Crystallogr., Sect. D* **2004**, *60* (9), 1679–1682.
(12) Kabsch, W. *J. Appl. Crystallogr.* **1993**, *26* (6), 795–800.
(13) Vagin, A.; Teplyakov, A. *J. Appl. Crystallogr.* **1997**, *30*, 1022–1025.
(14) Murshudov, G. N.; Vagin, A. A.; Dodson, E. J. *Acta Crystallogr., Sect. D* **1997**, *53* (3), 240–255.

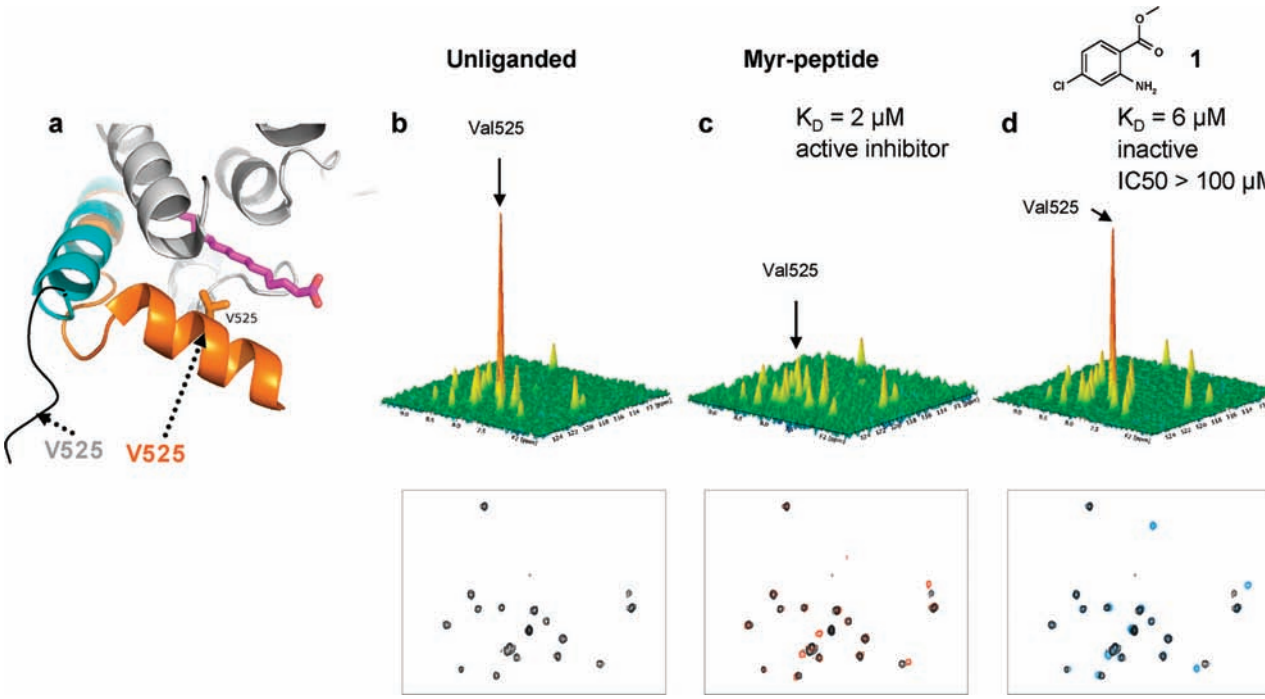

Figure 2. NMR-based conformational assay for helix_I. (a) Superposition of details around the myristate pocket from structures with an unliganded pocket (PDB code 2G2H, linear helix_I colored cyan) and with bound myristate (PDB code 1OPK, bent helix_I colored orange). (b−d) $^{15}N-^{1}H$ HSQC spectra of Abl/imatinib with unliganded myristate pocket, or complexed with the ligands shown on the top. The resonance of Val525 is indicated by the arrow.[10] Also given is the dissociation constant, K_D, as measured by NMR or ITC (see Supporting Information Figure 1), and the IC_{50} for inhibition of Bcr-Abl autophosphorylation in Bcr-Abl-transfected Ba/F3 cell lines. Contour plots of Abl/imatinib with unliganded myristate pocket (black) or complexed with Myr-peptide (red) or **1** (blue) is shown at the bottom.

using the molecular graphics program COOT[15] and maximum likelihood based minimization using Refmac5. Imatinib and the fragments were fitted to clear difference electron density, and then new water molecules were added using ARP/wARP[16] in the final cycles.

Results

Fragment-Based Screening. Fragment-based screening was carried out by NMR as a biophysical binding assay, using Abl kinase complexed with imatinib to block the active site. A small library containing 500 fragments was screened using T1ρ relaxation[17] and waterLOGSY[18] ligand observation experiments. Several hits were identified from our fragment library, most of them being non-kinase inhibitor scaffolds such as **1** or **2**. While most fragments were weak ligands, some of them bound surprisingly tightly for their low molecular weight ($K_D = 6$ and 22 μM for **1** and **2**, respectively; see Supporting Information Figure 1), yielding high ligand efficiencies and binding efficiency indices (0.59 and 28.2 for **1**, respectively). These hits were inactive in an Abl kinase biochemical assay, which was not surprising since only the kinase domain was used in the assay. However, all hits were also inactive in cell-based assays measuring either cell proliferation or autophosphorylation in Bcr-Abl-transfected Ba/F3 cell lines.[19] This was surprising since GNF-2 showed activity in these assays with an IC_{50} of 400 and 180 nM, respectively, and also the activity of weaker GNF-2 analogues could be detected up to IC_{50} values of >20 μM.

Why are biophysically validated Abl ligands not active inhibitors? This is explained by structural considerations: In order for the SH2 and SH3 domains to dock against the kinase domain and form the assembled inactive state, a conformational change is required for the C-terminal helix_I of the kinase domain, which has to bend toward the myristate pocket (Figure 1a,b). Crystal structures of Abl in complex with several fragments (Figure 1c,d), however, showed that binding of these fragments is incompatible with bending of helix_I due to potential steric clashes (e.g., with Ile521). Building a functional inhibitor by fragment-based screening thus requires starting points that allow or even induce helix_I to bend. Therefore, a rapid method to monitor the state of helix_I in Abl complexed with various ligands was required and was developed using NMR spectroscopy. We call this method a conformational assay because it detects a specific aspect of a protein conformation with the speed of a binding assay.

NMR-Based Conformational Assay. The NMR conformational assay requires ^{15}N-Val selectively labeled Abl kinase, which was economically prepared according to previously established protocols.[7] The conformational assay is based on different mobilities of Val525 in the two different conformational states (Figure 2a): with the myristate pocket in its unliganded state, helix_I is linear and ends with Ile521 (PDB code 1M52[21]), so that Val525 is unstructured and highly flexible and therefore leads to an intense NMR signal. With myristate

(15) Emsley, P.; Cowtan, K. *Acta Crystallogr., Sect. D* **2004**, *60* (12), 2126–2132.
(16) Perrakis, A.; Sixma, T. K.; Wilson, K. S.; Lamzin, V. S. *Acta Crystallogr., Sect. D* **1997**, *53* (4), 448–455.
(17) Hajduk, P. J.; Olejniczak, E. T.; Fesik, S. W. *J. Am. Chem. Soc.* **1997**, *119* (50), 12257–12261.
(18) Dalvit, C.; Fogliatto, G.; Stewart, A.; Veronesi, M.; Stockman, B. *J. Biomol. NMR* **2001**, *21* (4), 349–359.
(19) Weisberg, E.; et al. *Cancer Cell* **2005**, *7* (2), 129–141.
(20) Levinson, N. M.; Kuchment, O.; Shen, K.; Young, M. A.; Koldobskiy, M.; Karplus, M.; Cole, P. A.; Kuriyan, J. *PLoS Biol* **2006**, *4* (5), e144.
(21) Nagar, B.; Bornmann, W. G.; Pellicena, P.; Schindler, T.; Veach, D. R.; Miller, W. T.; Clarkson, B.; Kuriyan, J. *Cancer Res.* **2002**, *62* (15), 4236–4243.

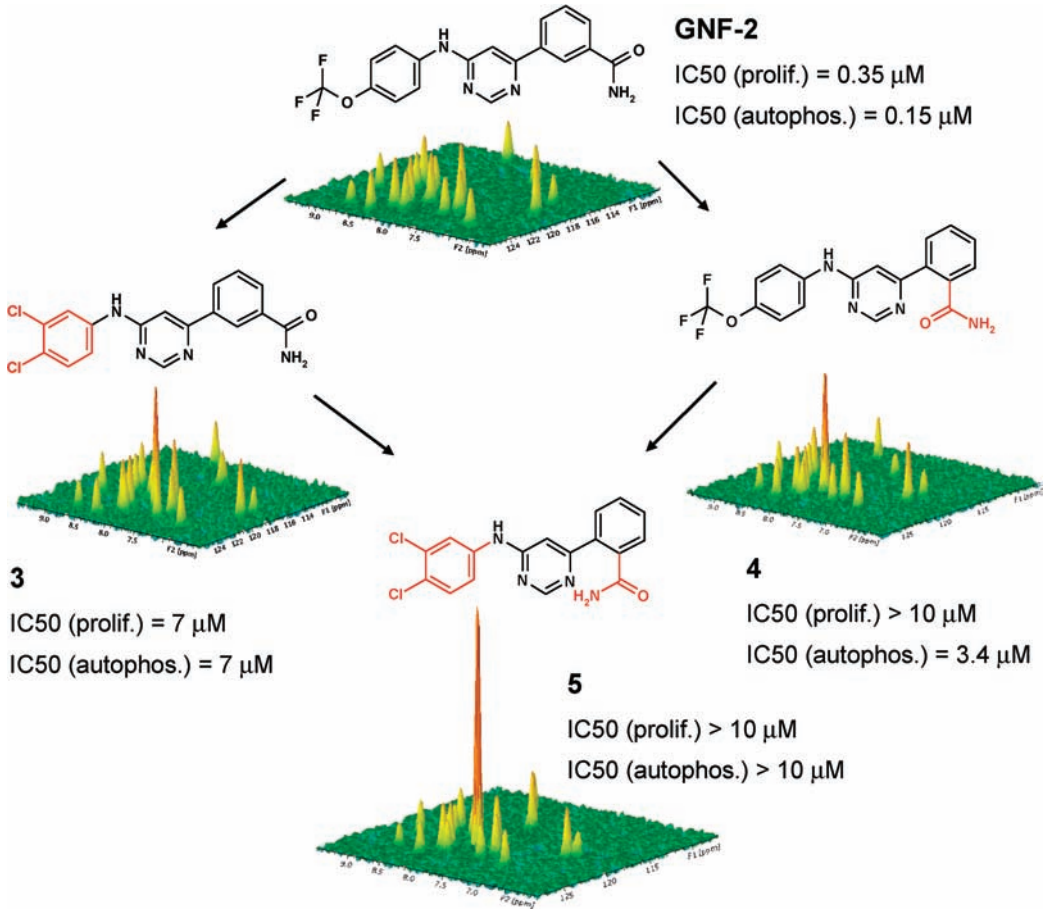

Figure 3. Structures, cellular activities, and conformational assay results for GNF-2 and close analogues. For contour plots, see Supporting Information Figure 2.

bound, Val525 is an integral part of helix_I′, is well-structured and ordered, and therefore has an NMR intensity equal to the intensities from the rest of the kinase. In this conformational assay, a strong Val525 NMR signal thus indicates a flexible and unbent helix_I, while average NMR signals indicate an ordered and bent helix_I. Intermediate intensities can result from various degrees of helix I bending and represent the time-averaged percentage of helix_I being in a linear or bent conformation.

Figure 2 displays NMR HSQC spectra of ^{15}N-Val-labeled Abl/imatinib with an unliganded myristate pocket (b), bound to a myristoylated peptide derived from the Abl N-terminus[2] (c), and bound to **1**, which has a K_D of 6 μM but no inhibitory activity up to 100 μM (d). The flexibility of Val525 in the linear conformation of helix_I (b) or in presence of a fragment that does not allow helix_I bending (d) can clearly be seen in Figure 2. In contrast, the reduction in flexibility upon helix_I bending induced by complexation with the Myr-peptide is shown in Figure 2c. Each spectrum is recorded within a few hours, does not require crystallization, and reflects solution conditions without crystal packing effects.

This conformational assay distinguishes ligands that merely bind to Abl kinase from ligands that bind and are functional inhibitors. The assay thus bridges the gap between binding and inhibition and is an indispensable flowchart assay for a fragment-based approach using biophysical screens.

Binding and Bending by GNF-2 Analogues. We applied this assay also to GNF-2 and close analogues in order to better understand the structure−activity relationships and the mechanism of inhibition. As expected, GNF-2 leads to complete bending of helix_I, consistent with its functional activity (Figure 3). Adrian et al.[5] point out the strict requirement for the 4-trifluoromethoxyaniline headgroup for the activity of GNF-2. We replaced this group by a dichloroaniline headgroup and confirmed a 20-fold activity decrease of the resulting compound **3** in cellular assays. However, we were surprised to see that compound **3** still binds to the myristate pocket of Abl with high affinity (Supporting Information Figure 2). The NMR conformational assay explained this observation by showing that, in complex with **3**, helix_I is not any more fully bent (Figure 3). Thus, the replacement of the 4-trifluoromethoxyaniline headgroup of GNF-2 does not lead to a compound that lacks binding affinity to Abl, but to a compound that cannot induce the conformational changes required for functional activity. Notably, there is no steric hindrance for helix_I in the bent conformation even with the dichloroaniline headgroup. Sterically, a bent helix_I would be possible but is energetically not favored.

Analysis of the Abl/GNF-2 crystal structure[6] predicts steric hindrance of the bent helix_I with a GNF-2 analogue having the amide in *ortho*- rather than *meta*-position. Indeed, compound **4** does not induce full bending of helix_I (Figure 3), and accordingly, its cellular activity is at least 20-fold reduced. Combining both changes (compound **5**) leads to a complete loss of helix bending and to inactivity in all cellular assays (Figure 3).

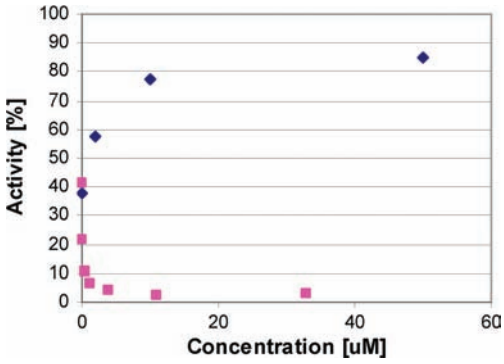

Figure 4. Abl inhibitors and activators. Dose−response of an Abl inhibitor (GNF-2, pink) and an Abl activator (**5**, blue) in a biochemical enzyme assay.

Allosteric c-Abl Agonists. A compound that binds to the myristate pocket but prevents helix_I from adopting the bent conformation should not be a functional inhibitor, but we hypothesized that it should still have functional activity. By competing with endogenous myristoyl groups, or with myristate mimetics, it should interfere with the autoinhibition of Abl, destabilize the assembled inactive state, and thus activate the kinase. Ligands binding to the Abl myristate pocket and inducing helix_I bending should be Abl antagonists, whereas ligands that bind but interfere with helix_I bending should be Abl agonists. Allosteric agonism by myristate ligands destabilizing the assembled inactive state resembles the G2A Abl mutant that lacks the myristoylation site and can therefore not form the assembled inactive state.[1] It also resembles the PP mutant where the assembled inactive state is destabilized by mutation of two prolines in the SH2-kinase linker.[22]

In order to test this hypothesis, a biochemical assay was developed using a c-Abl construct including the SH3, SH2, and kinase domains. In such an assay, the activity of myristate pocket ligands can be measured, and GNF-2 has an IC_{50} of 10 nM. In order to mimic the myristoylation of (unmyristoylated) c-Abl, the assay was run with the myristoylated c-Abl 1b peptide described in ref 1 at a concentration corresponding to its IC_{60}. Taking this as the intrinsic activity of naturally myristoylated c-Abl, all functional inhibitors decrease this activity in a dose-dependent manner. However, the Abl agonist **5**, a close analogue of GNF-2, actually increases c-Abl activity in a dose-dependent manner, demonstrating the allosteric agonism of myristate ligands that interfere with the conformational changes required for allosteric antagonism (Figure 4). Due to the role of c-Abl in DNA damage repair,[23] c-Abl (not Bcr-Abl) activators may have a therapeutic benefit after radiation therapy. Moreover, recent data suggest that c-Abl activators can block TGFβ-responsive mammary tumor growth in mice.[24]

Discussion

Recently, Bcr-Abl inhibitors that bind to the myristate pocket were identified.[5] Since the screen was using a cellular assay, they are functional inhibitors that lead to potent inhibition of the kinase. However, our study used a biophysical screen and showed that ligands for the myristate pocket are not necessarily functional inhibitors. Using a conformational assay, we showed that only those myristate ligands are functional inhibitors that bend helix_I, thus differentiating "bending" from mere "binding". Moreover, we showed that ligands that "bind" without "bending" interfere with the autoinhibition of Abl and activate the kinase. To our knowledge, this is the first report of small molecules influencing the position of a crucial kinase helix that determines agonism or antagonism and of a biophysical assay to detect these conformational changes. Previous NMR-based assays were either binding assays (possibly giving information about the binding site) or activity assays,[25,26] but the concept of a conformational assay is novel. It closes the gap between binding and inhibition for allosteric kinase ligands and expands the utility of NMR spectroscopy in drug discovery.[27]

Pharmaceutical research in the past has focused on kinase inhibitors. The therapeutic potential of kinase activators has received little attention, and only few examples for kinase activators are known,[28−30] some of them indirect and unintended.[31−33] This is likely due to the fact that the discovery of kinase inhibitors is more straightforward than the discovery of kinase activators: essentially any ligand that binds to the active site inhibits kinase activity by blocking the access of substrate. In contrast, kinase activators must bind outside of the active site to stabilize the active conformation or interfere with kinase autoinhibition. Suitable binding sites for such activators may not always be present and have to be identified individually for each kinase. Since in contrast to the ATP binding pocket, such allosteric sites are nonconserved, classical chemical matter targeted for kinase active sites may not yield potent hits, and alternative methods such as fragment-based screening may be needed to identify suitable starting points. Since tool compounds are rarely available to optimize biochemical or cellular assays for the detection of kinase activators, biophysical screens can help to generate such tool compounds, as in the current study. Due to the nonconserved nature of allosteric binding pockets, allosteric kinase modulators have potential to reach a high degree of selectivity. Given the role of Bcr-Abl in CML and other diseases, and the therapeutic benefit of Bcr-Abl inhibitors such as imatinib, nilotinib, and dasatinib, an interest in activators seems paradoxical at first glance. However, c-Abl (in contrast to Bcr-Abl) does have beneficial effects, for example, in DNA damage repair, and c-Abl (not Bcr-

(22) Barila, D.; Superti-Furga, G. *Nat. Genet.* **1998**, *18* (3), 280–282.
(23) Raina, D.; Pandey, P.; Ahmad, R.; Bharti, A.; Ren, J.; Kharbanda, S.; Weichselbaum, R.; Kufe, D. *J. Biol. Chem.* **2005**, *280* (12), 11147–11151.
(24) Allington, T. M.; Galliher-Beckley, A. J.; Schiemann, W. P. *FASEB J.* **2009**, *23* (12), 4231–4243.
(25) Shuker, S. B.; Hajduk, P. J.; Meadows, R. P.; Fesik, S. W. *Science* **1996**, *274* (5292), 1531−1534.
(26) Dalvit, C. *Prog. Nucl. Magn. Reson. Spectrosc.* **2007**, *51* (4), 243–271.
(27) Jahnke, W. *J. Biomol. NMR* **2007**, *39* (2), 87–90.
(28) Li, S.; Covino, N. D.; Stein, E. G.; Till, J. H.; Hubbard, S. R. *J. Biol. Chem.* **2003**, *278* (28), 26007–26014.
(29) Hindie, V.; Stroba, A.; Zhang, H.; Lopez-Garcia, L. A.; Idrissova, L.; Zeuzem, S.; Hirschberg, D.; Schaeffer, F.; Jorgensen, T. J.; Engel, M.; Alzari, P. M.; Biondi, R. M. *Nat. Chem. Biol.* **2009**, *5* (10), 758–764.
(30) Zhang, X.; Gureasko, J.; Shen, K.; Cole, P. A.; Kuriyan, J. *Cell* **2006**, *125* (6), 1137–1149.
(31) Heidorn, S. J.; Milagre, C.; Whittaker, S.; Nourry, A.; Niculescu-Duvas, I.; Dhomen, N.; Hussain, J.; Reis-Filho, J. S.; Springer, C. J.; Pritchard, C.; Marais, R. *Cell* **2010**, *140* (2), 209–221.
(32) Cameron, A. J.; Escribano, C.; Saurin, A. T.; Kostelecky, B.; Parker, P. J. *Nat. Struct. Mol. Biol.* **2009**, *16* (6), 624–630.
(33) Okuzumi, T.; Fiedler, D.; Zhang, C.; Gray, D. C.; Aizenstein, B.; Hoffman, R.; Shokat, K. M. *Nat. Chem. Biol.* **2009**, *5* (7), 484–493.

Abl) activators could have therapeutic benefit after radiation therapy.[23] Recent studies even suggest a direct protective effect of c-Abl against TGFβ-responsive mammary tumor growth.[24] The present publication is one of very few reports on kinase activators and the first report of a c-Abl activator, and it will be interesting to see further applications of kinase activators.

A recent report on synergistic effects of a combination of allosteric and ATP-directed Bcr-Abl inhibitors suggests new pharmacological opportunities to overcome resistance against current Bcr-Abl inhibitors,[6] but the first inhibitors are rarely the ones with the best overall profile. Our basic understanding of allosteric Abl inhibition and the conformational assay to detect the required structural changes now paves the way for a rational design of novel allosteric Abl inhibitors with improved pharmacological properties.

Acknowledgment. We thank Drs. Markus Warmuth and Nathanael Gray for helpful discussions, Anke Blechschmidt for ITC measurements, Janis Liebetanz for the c-Abl clone, Navratna Vajpai and Stephan Grzesiek for resonance assignment work, and Chrystèle Henry, Gabriele Rummel, Robert Kastl, and Dominique Kempf for expert technical assistance.

Supporting Information Available: Titration curves for fragments **1** and **2**, contour plots for Figure 3, synthesis of compounds **3**−**5**, crystallographic data, and complete refs 6 and 19. This material is available free of charge via the Internet at http://pubs.acs.org. All of the crystal structures with fragments described in this paper have been deposited in the Protein Data Bank (PDB codes 3MS9 and 3MSS).

JA101837N